Supplementary Information

Structural Confinement Engineering of Current Collectors Enables Durable SiOx Anodes for Lithium-Ion Batteries

Raehyeong Lee[a], Jinyeong Choi[a], Soojin Choi[a], Ah Reum Choi lee[e], Jin Hong lee[c, d, e,*], Jae Ho Kim[a, b, c, d,*], Minjoon Park[a, b, c, d,*]

[a]Department of Nano Fusion Technology, Pusan National University, Busan daehak-ro 63 beon-gil 2, Geumjeong-gu, Busan, 46241, Republic of Korea
[b]Advanced Energy Major, School of Transdisciplinary Engineering, Pusan National University, Busan daehak-ro 63 beon-gil 2, Geumjeong-gu, Busan, 46241, Republic of Korea
[c]Research Center of Energy Convergence Technology, Pusan National University, Busandaehak-ro 6 3beon-gil 2, Geumjeong-gu, Busan, 46241, Republic of Korea
[d]Eco-friendly Battery Engineering, Pusan National University, Busandaehak-ro 63beon-gil 2, Geumjeong-gu, Busan, 46241, Republic of Korea
[e]School of Chemical Engineering, Pusan National University, 46241, Busandaehak-ro 63beon-gil 2, Geumjeong-gu, Busan, 46241, Republic of Korea
E-mail: jinhong.lee@pusan.ac.kr, jhkim8@pusan.ac.kr, mjpark@pusan.ac.kr

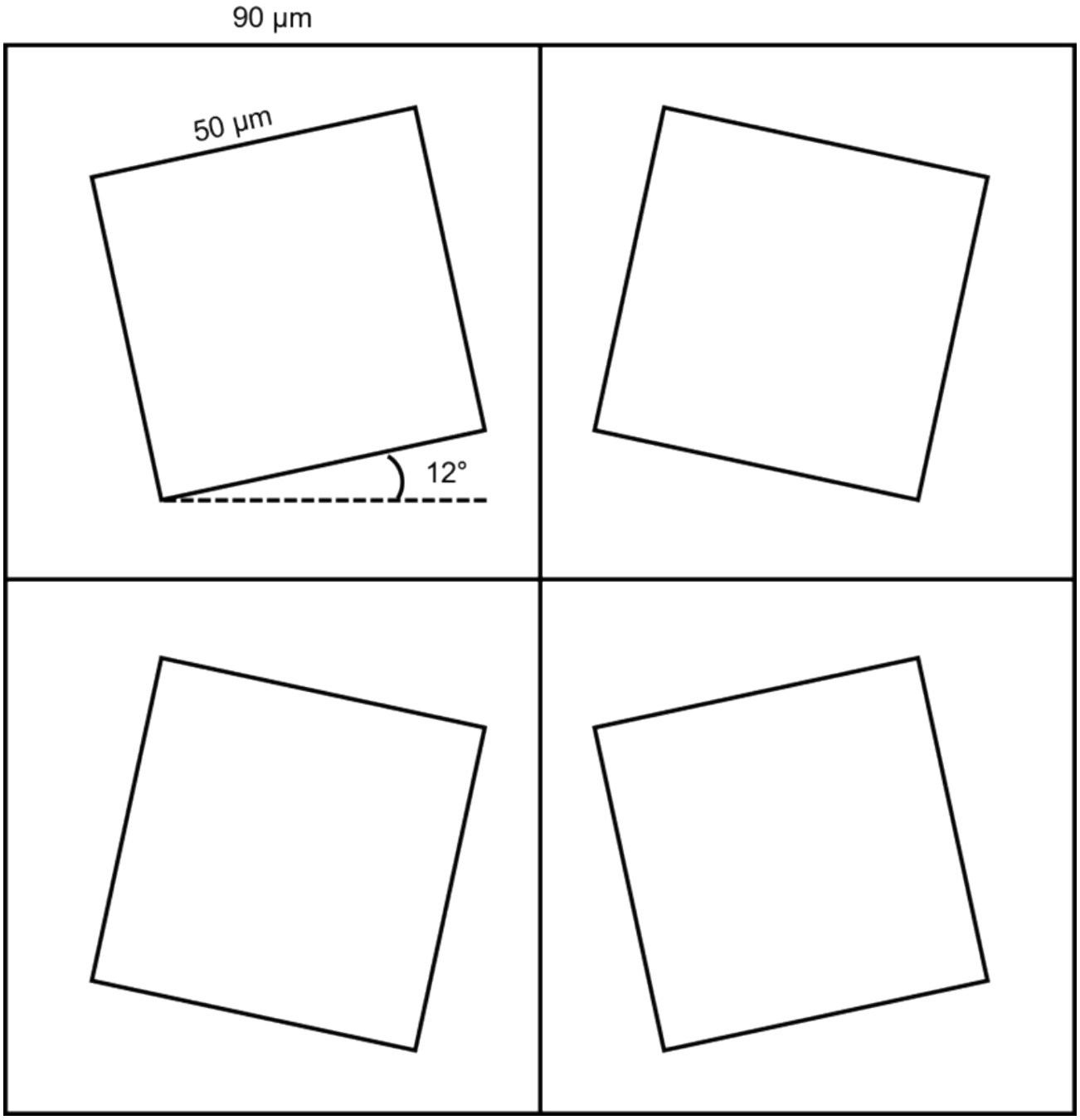

Fig. S1. Structure details of SPCM.

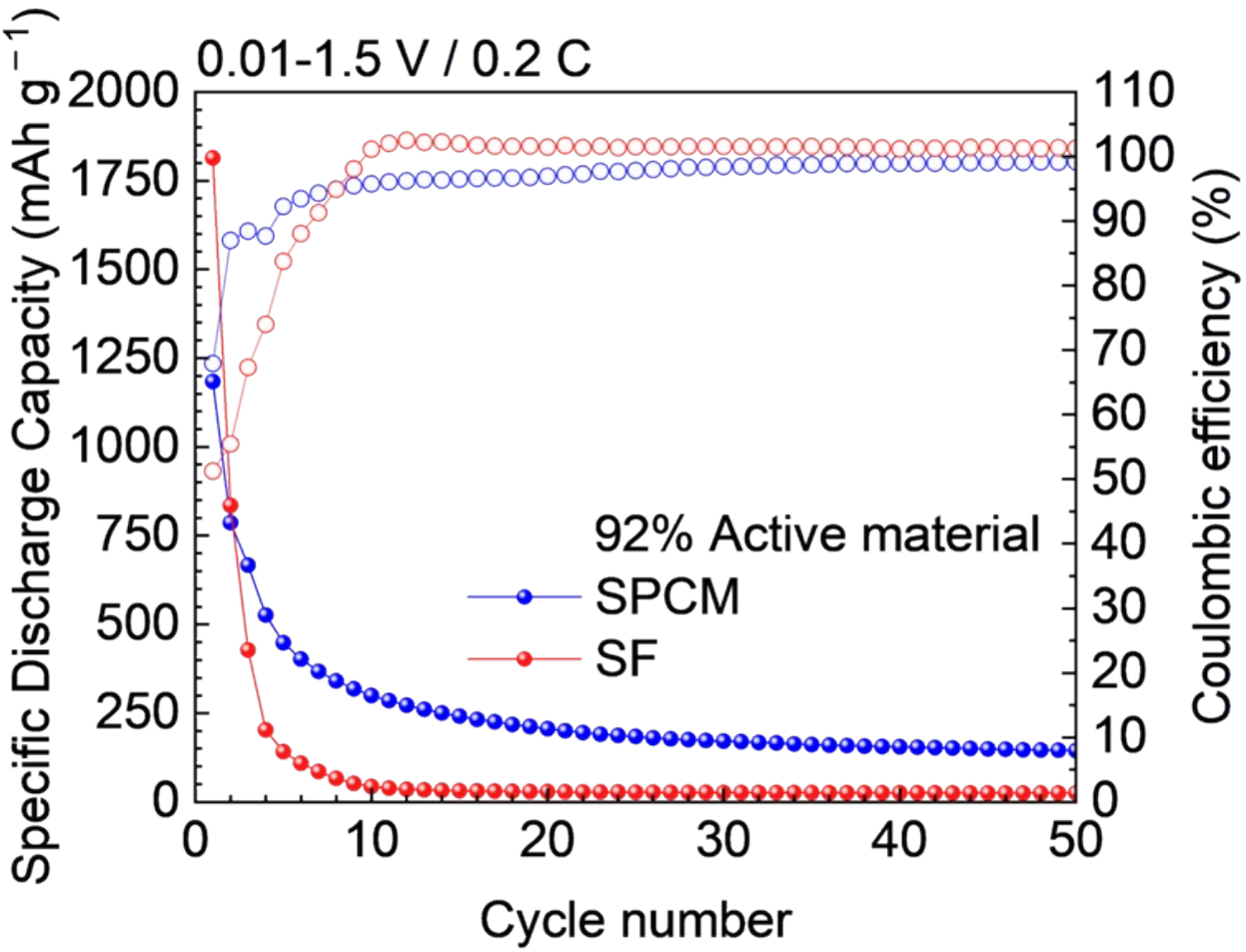

Fig. S2. Cycling performance of SF and SPCM containing 92% active material.

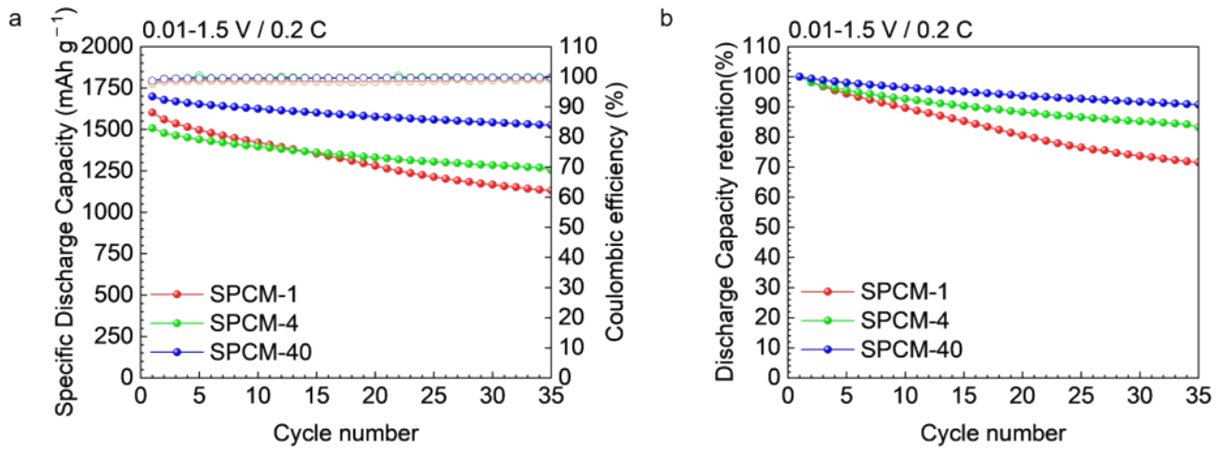

Fig. S3. (a) Cycling performance profiles of SPCM-1, SPCM-4 and SPCM-40 at 0.2 C. (e) Capacity retention profiles of SPCM-1, SPCM-4 and SPCM-40 at 0.2 C.

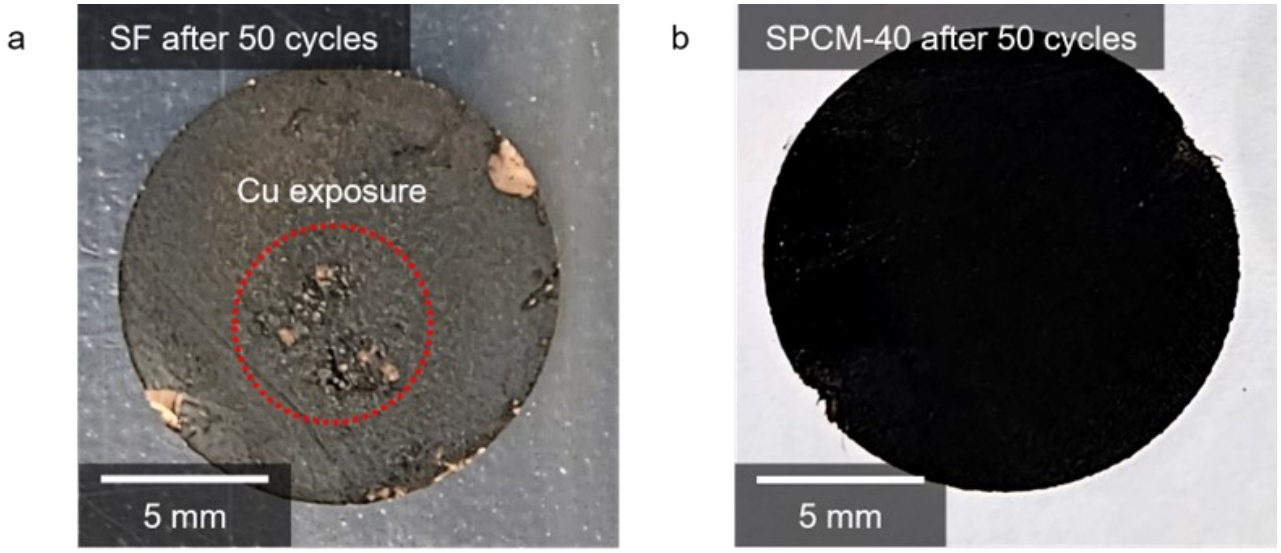

Fig. S4. Images of (a) SF electrode and (b) SPCM-40 electrode after degradation.

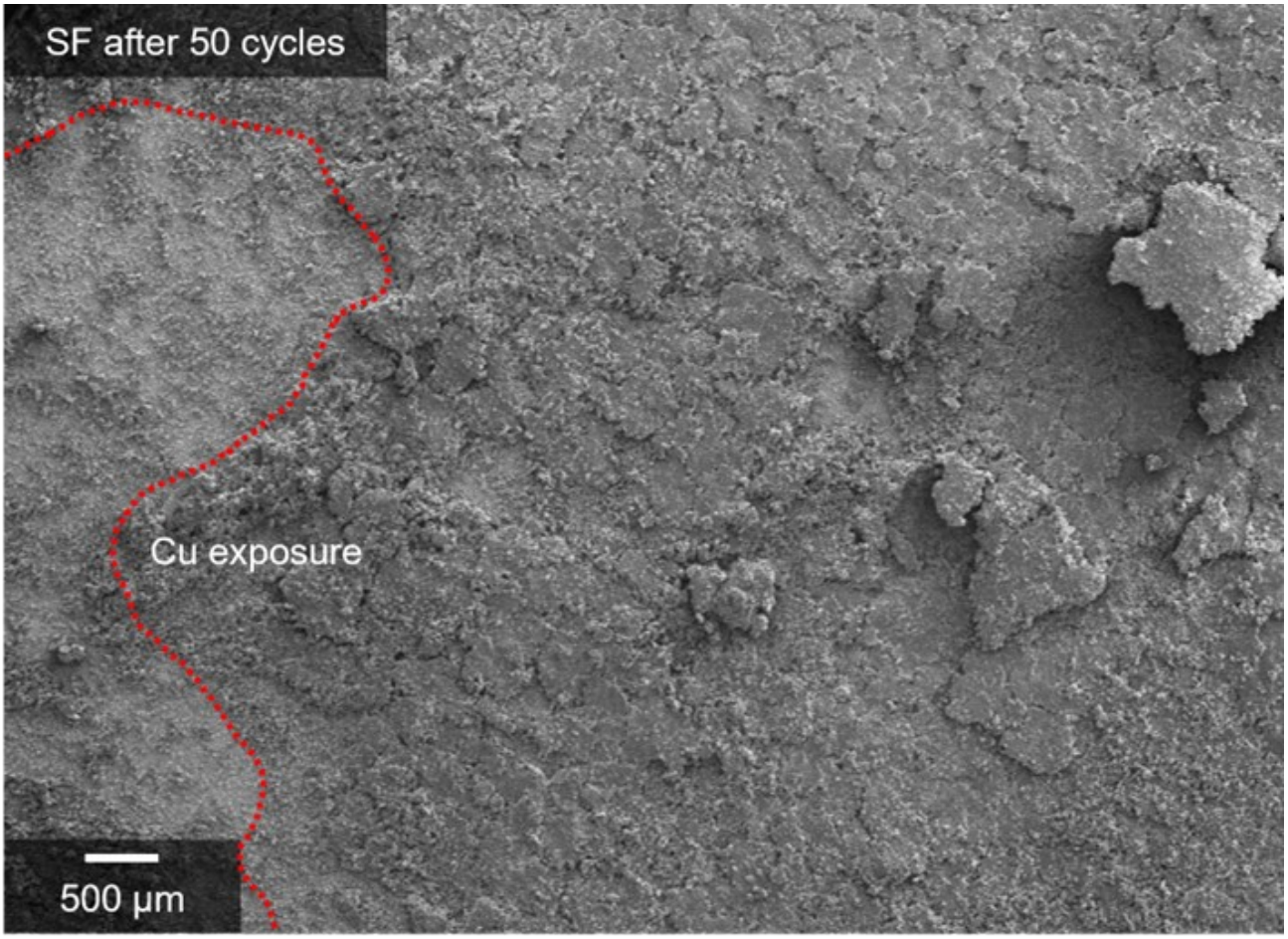

Fig. S5. Low magnified SEM image of SF after degradation.

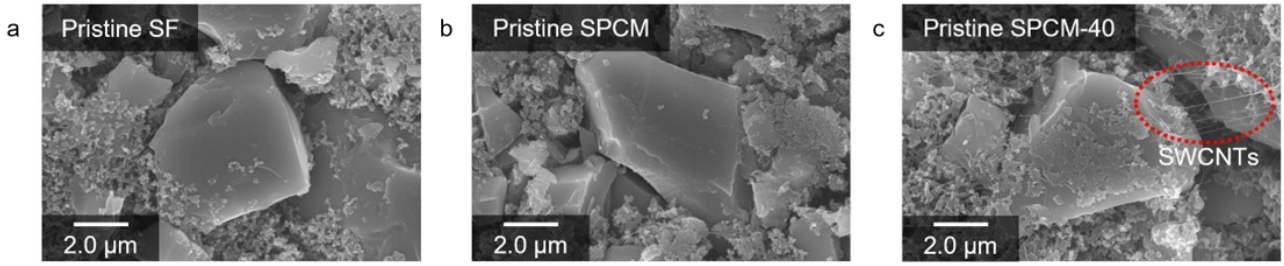

Fig. S6. SEM images of SiOx particles in (a) SF, (b) SPCM, and (c) SPCM-40 before degradation,

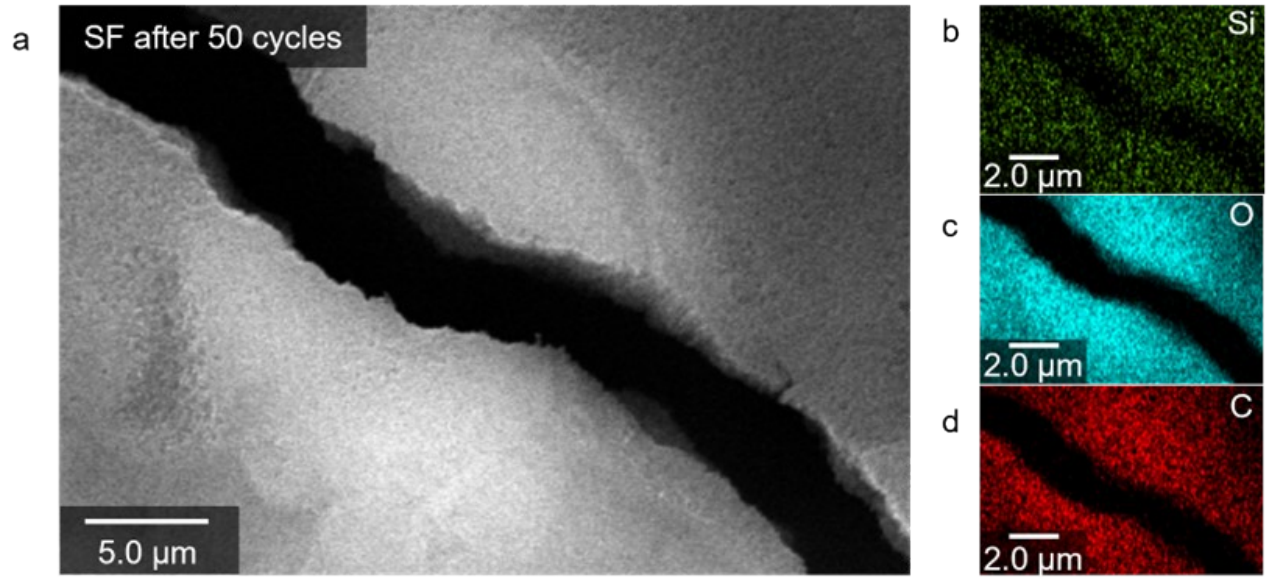

Fig. S7. (a) SEM image, and (b-d) EDS mappings of SF. (b) Si $K\alpha_1$ elemental maps. (c) O $K\alpha_1$ elemental maps. (d) C $K\alpha_1$ elemental maps.

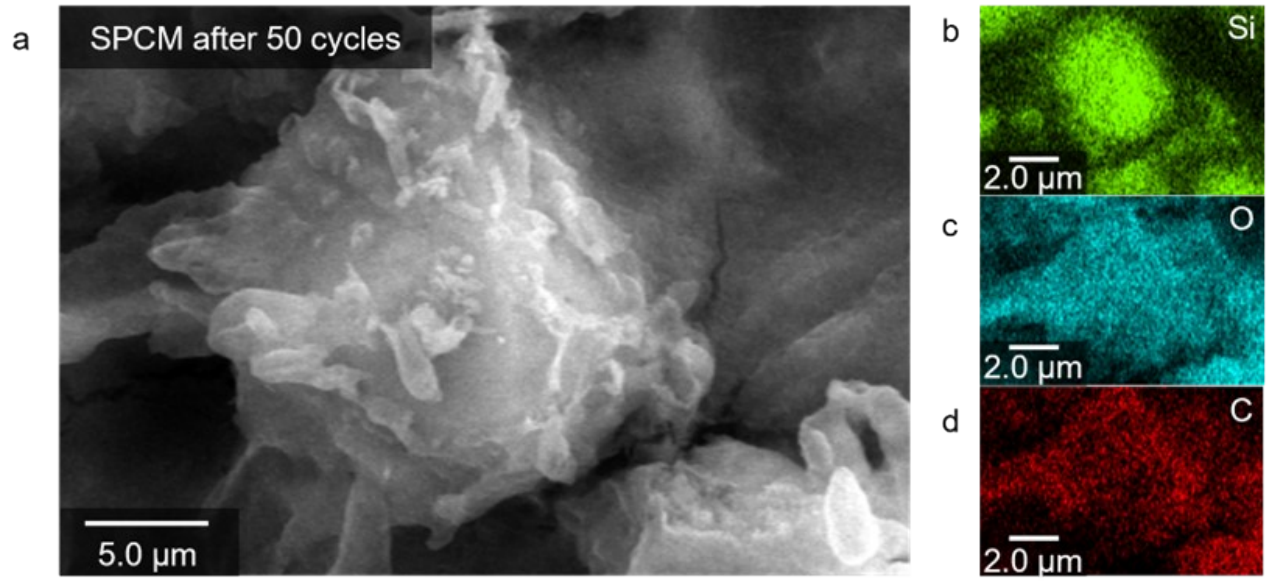

Fig. S8. (a) SEM image, and (b-d) EDS mappings of SPCM. (b) Si $K\alpha_1$ elemental maps. (c) O $K\alpha_1$ elemental maps. (d) C $K\alpha_1$ elemental maps.

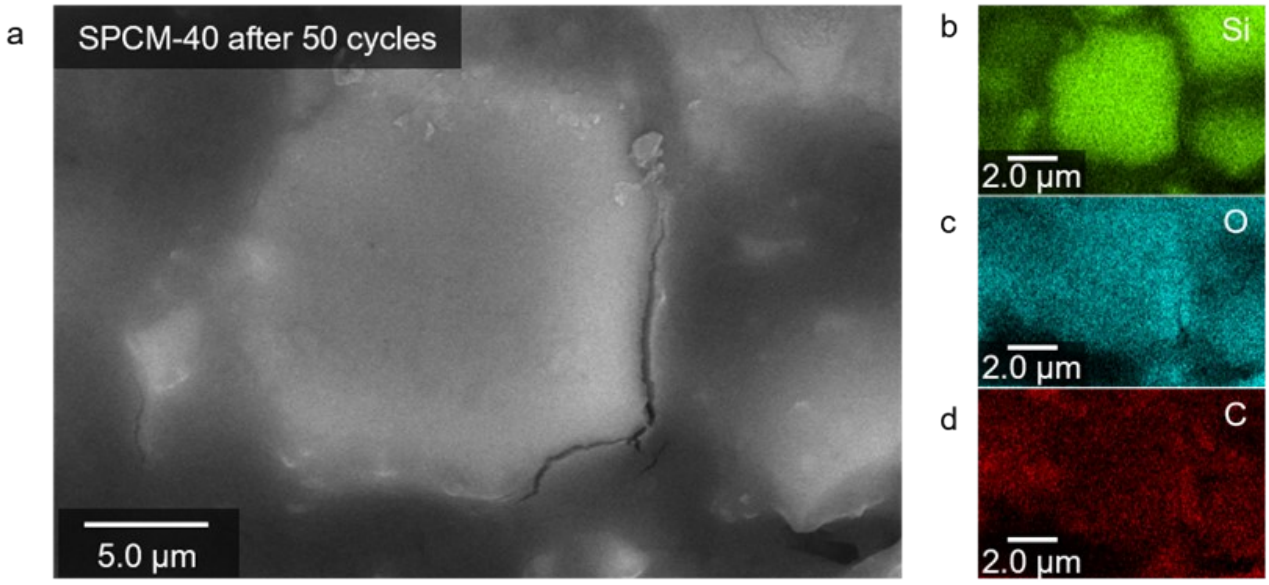

Fig. S9. (a) SEM image, and (b-d) EDS mappings of SPCM-40. (b) Si $K\alpha_1$ elemental maps. (c) O $K\alpha_1$ elemental maps. (d) C $K\alpha_1$ elemental maps.

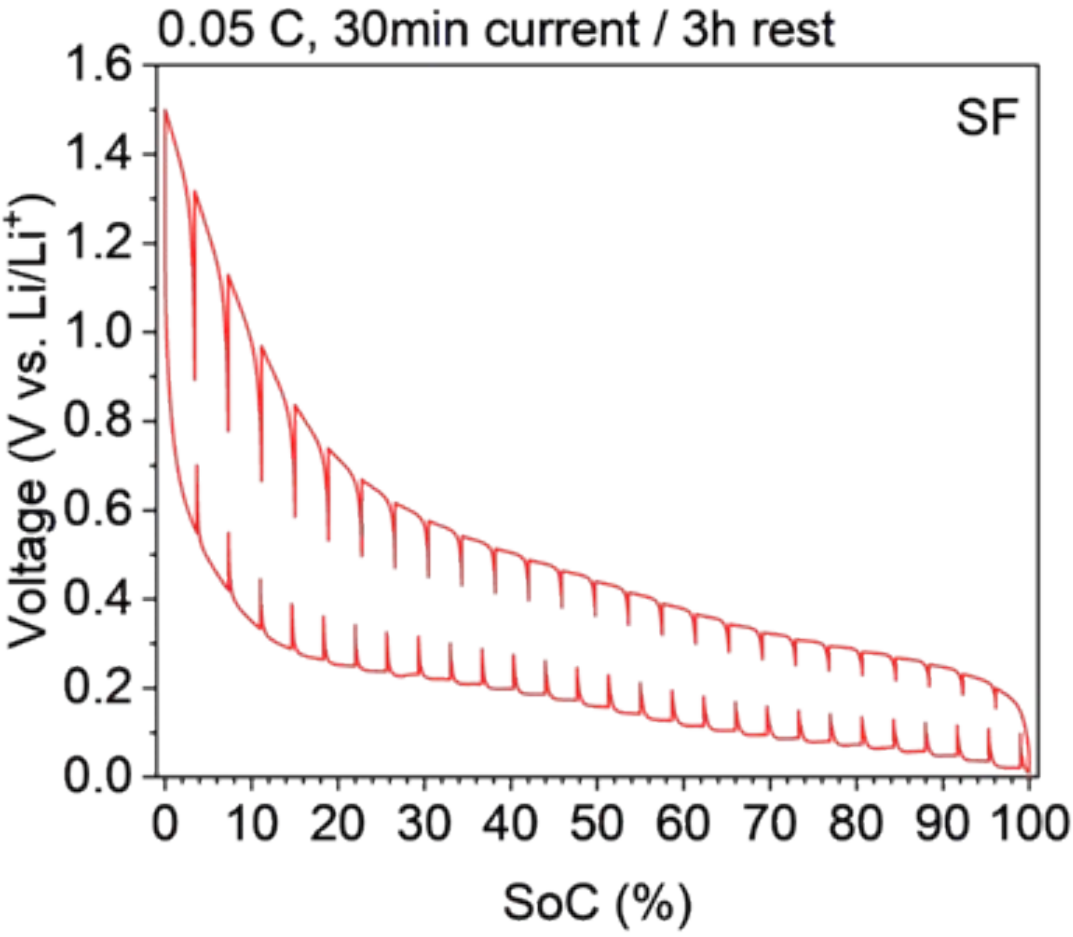

Fig. S10. GITT profile of SF.

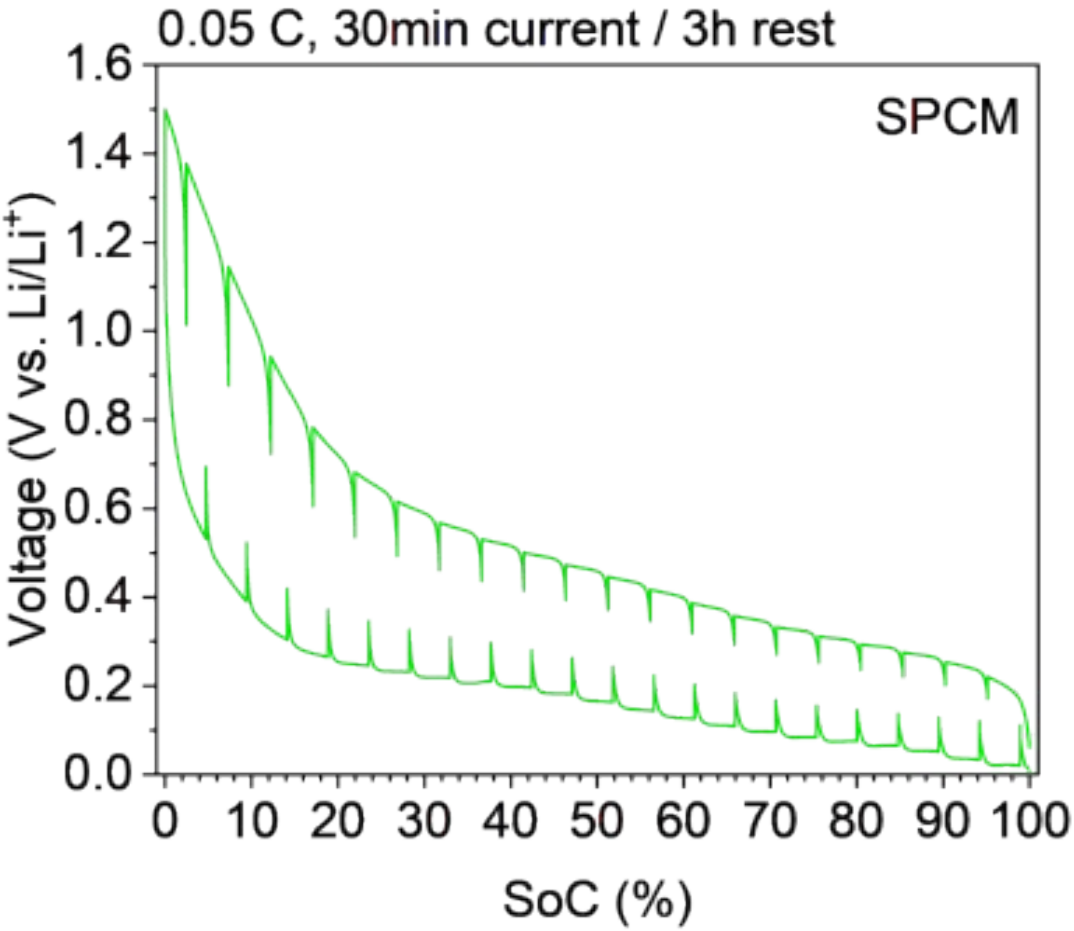

Fig. S11. GITT profile of SPCM.

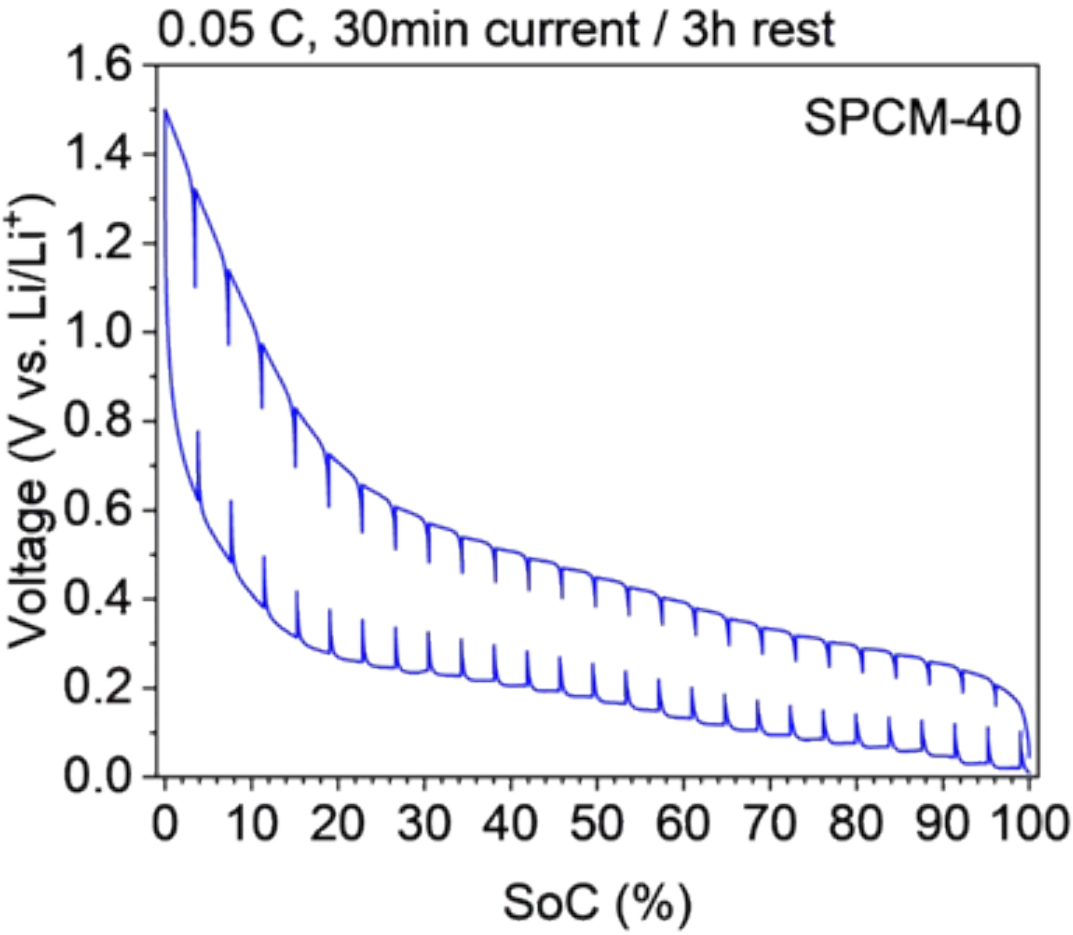

Fig. S12. GITT profile of SPCM-40.

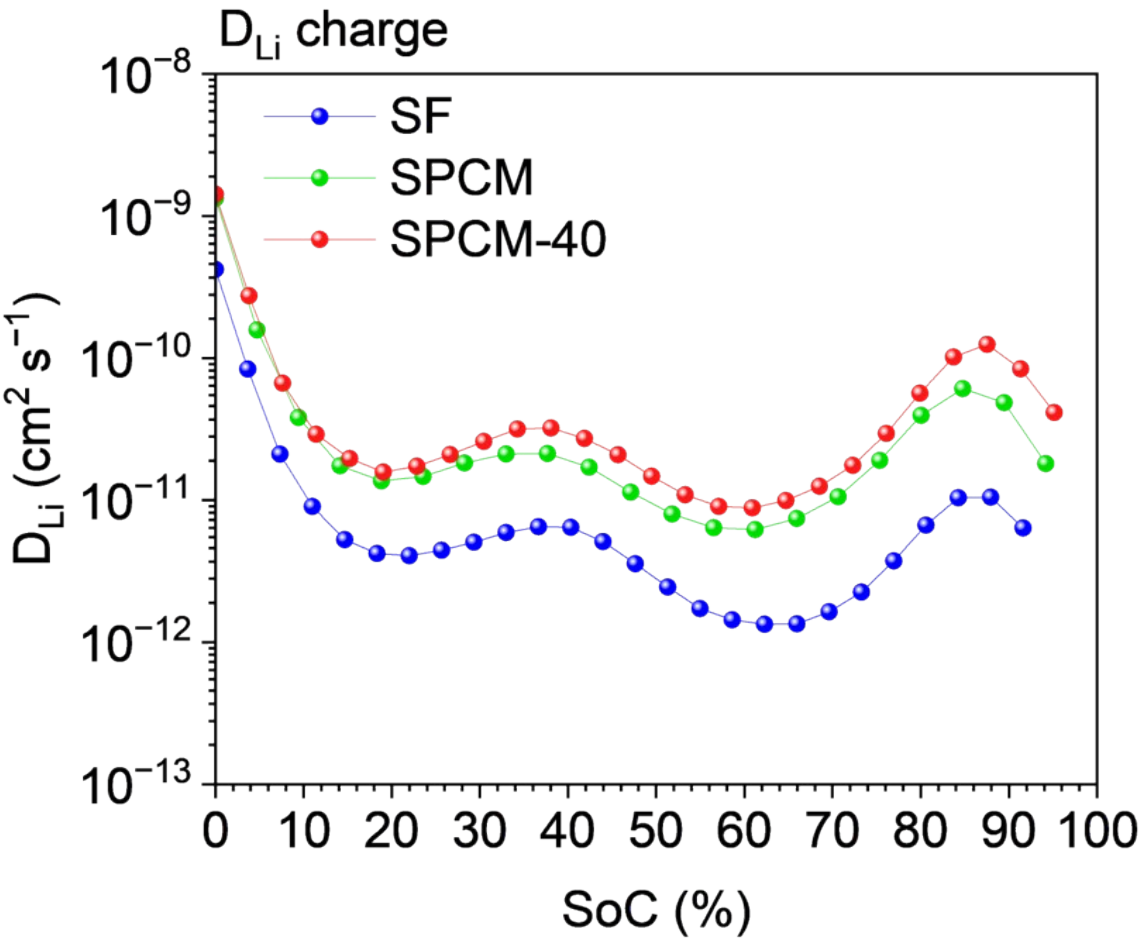

Fig. S13 Lithium-ion diffusion coefficient profiles of SF, SPCM, SPCM-40 calculated form GITT profiles under the charge process.

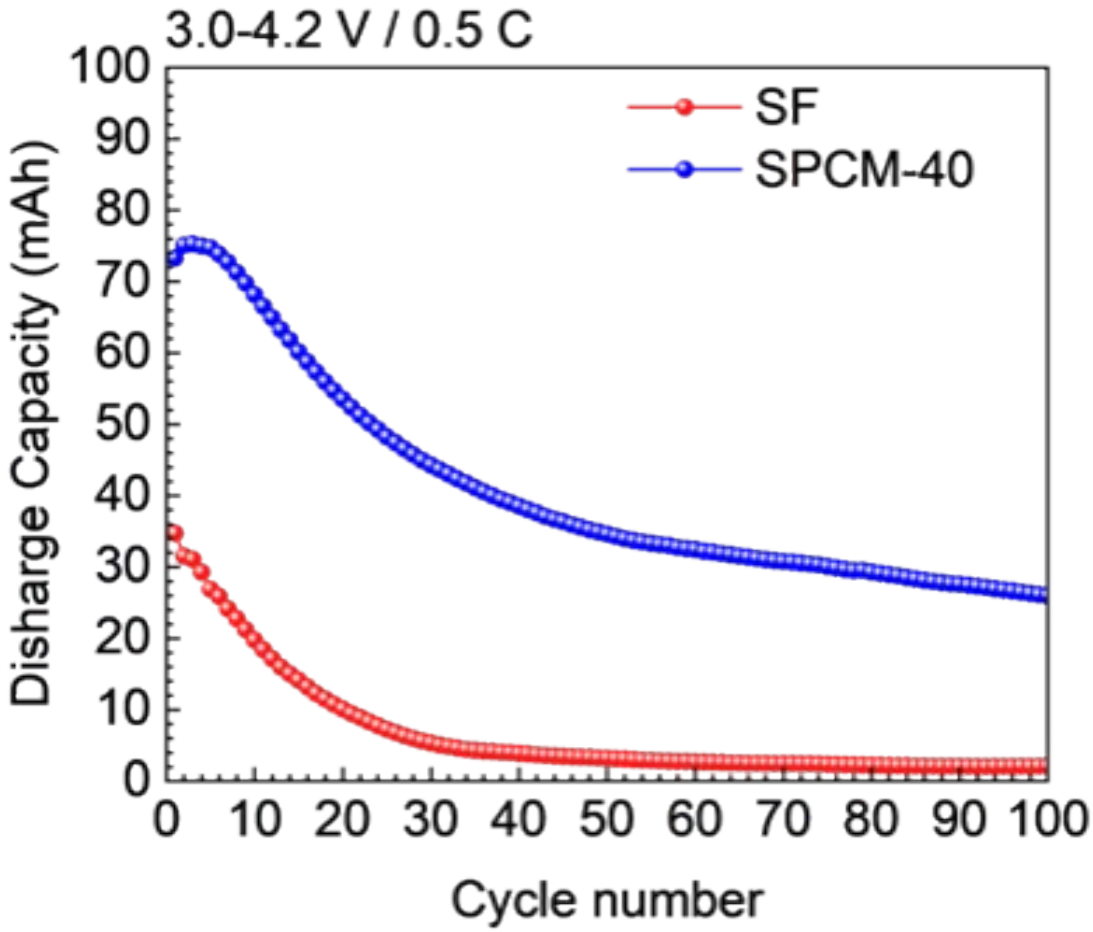

Fig. S14 Cycling performance profiles of SF and SPCM-40 pouch cells.